Lessons on textile history and fibre durability from a 4,000-year-old Egyptian flax yarn

Alessia Melelli, Darshil Shah, Gemala Hapsari, Roberta Cortopassi, Sylvie Durand, Olivier Arnould, Vincent Placet, Dominique Benazeth, Johnny Beaugrand, Frédéric Jamme, et al.

Lessons on textile history and fibre durability from a 4,000-year-old Egyptian flax yarn

Alessia Melelli[1], Darshil U. Shah[2], Gemala Hapsari[3], Roberta Cortopassi[4], Sylvie Durand[5], Olivier Arnould[6], Vincent Placet[3], Dominique Benazeth[4], Johnny Beaugrand[5], Frédéric Jamme[7] and Alain Bourmaud[1]✉

Flax has a long and fascinating history. This plant was domesticated around 8,000 BCE[1] in the Fertile Crescent area[2], first for its seeds and then for its fibres[1,3]. Although its uses existed long before domestication, residues of flax yarn dated 30,000 years ago have been found in the Caucasus area[4]. However, Ancient Egypt laid the foundations for the cultivation of flax as a textile fibre crop[5]. Today flax fibres are used in high-value textiles and in natural actuators[6] or reinforcements in composite materials[7]. Flax is therefore a bridge between ages and civilizations. For several decades, the development of non- or micro-destructive analysis techniques has led to numerous works on the conservation of ancient textiles. Non-destructive methods, such as optical microscopy[8] or vibrational techniques[9,10], have been largely used to investigate archaeological textiles, principally to evaluate their degradation mechanisms and state of conservation. Vibrational spectroscopy studies can now benefit from synchrotron radiation[11] and X-ray diffraction measurement in the archaeometric study of historical textiles[12,13]. Conservation of mechanical performance and the ultrastructural differences between ancient and modern flax varieties have not been examined thus far. Here we examine the morphological, ultrastructural and mechanical characteristics of a yarn from an Egyptian mortuary linen dating from the early Middle Kingdom (Eleventh Dynasty, ca. 2033–1963 BCE) and compare them with a modern flax yarn to assess the quality and durability of ancient flax fibres and relate these to their processing methods. Advanced microscopy techniques, such as nano-tomography, multiphoton excitation microscopy and atomic force microscopy were used. Our findings reveal the cultural know-how of this ancient civilization in producing high-fineness fibres, as well as the exceptional durability of flax, which is sometimes questioned, demonstrating their potential as reinforcements in high-technology composites.

The most beautiful fabric pieces of flax date from Ancient Egypt (Fig. 1), their highly preserved state a result of their optimal conservation over millennia in coffins or tombs with remarkably stable moisture and thermal conditions, as well as sheltering from UV light. Flax textiles were particularly prized by the Egyptians because of their comfort and the fineness of their fibres[14]. Flax was widely used for clothing (Fig. 1a) and in the fishing sector for work clothes, felucca sails and nets. The funerary uses included mummy strips (Fig. 1b), funeral linen (Fig. 1c,d,g) as well as ornaments (Fig. 1e).

In terms of cultivation, the fertile Nile valley with its light and rich sandy soils was particularly suitable for flax. After growing, the stems were pulled out, as shown in illustrations found in the tomb of Sennedjem (Deir el Medineh, Egypt) and then probably water-retted. Over the past century or so, growth conditions have changed and varietal selection has significantly increased the crop's fibre yields[15]. It is therefore difficult to compare varieties across the ages. Even so, an in-depth study of 407 flax genotypes of different origins has shown that regions that have been the centre of origin of the crop, such as the Mediterranean or Abyssinia, highlight haplotypes that are more unique than the temperate group and are representative of oil-seed plants[16]. The flax found in the lake dwelling does not belong to the species now cultivated (*Linum usitatissimum L*) but to *Linum angustifolium*[17], which is not cultivated at the present time. Today's cultivated flax *Linum usitatissimum* L. is considered as being domesticated from the wild progenitor pale flax *Linum angustifolium* Huds. Both have phenotypic characters of great heritability and are distinguishable by several characteristics, such as the length and width of petals, size of seeds, colour and shape of the flower, height of plants, but also the number of days until emergence from the soil or flowering[18]. However, the height of the plants shown on the Egyptian bas-reliefs[19] and the size of the seeds found during excavation[1] suggest that the species cultivated by the Egyptians were morphologically close to those we know today.

Figure 2a,d compare the overall architecture, observed by scanning electron microscopy (SEM), of old (Fig. 1g and Supplementary Fig. 1a) and modern (Supplementary Fig. 1b) flax yarn, respectively. Despite a lower level of twist (about 180 turns per metre (tpm) against 320 tpm for the modern flax), the old flax possesses a similar metric number (about 122 tex or 8.2 km kg^{-1}), showing the mastery of the Egyptians in manual spinning. Figure 2b reveals the level of individualization of the fibres. In the flax stem, fibres are aggregated in cohesive bundles made of several tens of fibres, the fibres being more or less divided after retting and extraction stages. The old yarn is mainly made up of elementary flax fibres; the residues of cortical parenchyma and middle lamellae are very few. This demonstrates the effectiveness of the water-retting process utilized at the time as Pliny the Elder explained[20]. Water-retting enables homogeneous retting and, when it is well executed, enables the production of very fine fibres. One can notice that the low fibre yield in ancient flax varieties can also lead to easier retting and fibre division[21]. In modern flax fibre extraction processes, stems undergo field retting over

[1]Univ. Bretagne Sud, UMR CNRS 6027, IRDL, Lorient, France. [2]Centre for Natural Material Innovation, Department of Architecture, University of Cambridge, Cambridge, UK. [3]FEMTO-ST Institute, Department of Applied Mechanics, UMR CNRS 6174, University of Franche-Comté, Besançon, France. [4]Musée du Louvre, Département des Antiquités Egyptiennes, Paris, France. [5]INRAE, UR1268 BIA Biopolymères Interactions Assemblages, Nantes, France. [6]LMGC, Université de Montpellier, UMR CNRS 5508, Montpellier, France. [7]Synchrotron SOLEIL, DISCO beamline, Gif-sur-Yvette, France. ✉e-mail: alain.bourmaud@univ-ubs.fr

Fig. 1 | Examples of the uses of flax in ancient Egypt. a, Child's vest with dyed blue edges, 800–720 or 700–540 BCE. **b**, Mummy of man with agglomerated and stuccoed flax fabric, 332–30 BCE. **c**, Flax hypocephalus, 305–30 BCE. **d**, Fragment of flax shroud, 1550–1295 BCE. **e**, Hairnet cap, fifth or sixth century AD. **f**, Unspun flax hank, 1420–1230 BCE. **g**, Mortuary linen, 2140–1976 BCE. Objects in **c** and **d** are exposed at the British Museum (London, UK); **b** is exposed and **a**, **e**, **f** and **g** are in the store room at Le Louvre Museum (Paris, France). All images are from the authors' personal collection. Images of objects in **a**, **e**, **f** and **g** were obtained with the specific permission of Le Louvre Museum.

several weeks. Dependent on natural weather conditions, this can lead to retting heterogeneity. As a consequence, numerous residues of pectic intermediate lamellae or cortical parenchyma are visible on the modern flax yarn (Fig. 2e,h). Such residues increase roughness of the yarn and are detrimental to the sensation of comfort (for example softness). This contrasts with the reputation of Egyptian flax fabrics, the most beautiful specimens of which were reserved for members of high society. These observations validate the important know-how of ancient Egyptians in textile manufacturing. The scanning electron micrographs (Fig. 2a,b) also reveal the excellent general conservation of the ancient fibrous yarns.

Figure 2g,h present cross-sections of the old and the modern yarn observed in nano-tomography and Fig. 2i illustrates the analysed distribution of elementary fibre diameters for the two materials. The mean diameters were $14.3 \pm 3.3\,\mu m$ for the fibres in the old yarn ($n = 523$) and $17.6 \pm 3.6\,\mu m$ for the modern yarn ($n = 208$); both diameter values are consistent with typically reported values on flax fibres[22]. A significant difference in elementary fibre diameters was observed and confirmed by a Student's *t*-test with $P \leq 0.001$. The smaller diameters of old flax may be related to the plant variety, the weather conditions during growth (hydric stress, for example)[23] and/or even the sampling area within the stem, with larger diameter fibres being generally located in the middle section of the stem height[24]. The retting method utilized may also explain the differences and scatter in elementary fibre diameters between the old and the modern flax yarn (Fig. 2i). The use of water-retting for the old flax yarn leads to completely separated fibres that are free from surface residues (Fig. 2b). This further demonstrates the skill of ancient Egyptians in obtaining fine yarns and textiles.

Differences are also visible in the size of the lumens, with SEM and tomographic images (Fig. 2c,f–h) showing larger lumens for old flax fibres. While the lumens of modern flax fibres represent only a few percent of the total surface area[25], old fibres studied here possess lumens of the order of 30–40%, comparable to wood or coconut fibres[25]. We hypothesize that the low wall thickness of old flax may be due to a premature halt in the cellulose filling process of the cell walls following the intrusive growth phase[24]. This filling can be interrupted by extreme weather conditions, such as lodging or marked periods of hydric stress[26].

Flax fibres are characterized by their multilayered structure, their generally polygonal shape and the presence of structural defects known as kink-bands[27] distributed along the fibre length. Notably, the relative quantity and size of these kink-bands are particularly large on old fibres (Figs. 2b and 3a,b) in comparison with modern fibres (Fig. 3d,e). The origin of these defects is not well known, but the plant fibre community generally attributes them to mechanical stresses induced during the extraction or processing of the stems, as well as residual stresses that may be released during periods of stem or fibre drying, possibly during the retting stage[27,28]. The large quantity of kink-bands on old flax fibres may be the result of aggressive decortication, scutching or spinning processes used by the Egyptians following water-retting, but may also be caused by progressive release of internal stresses over the four millennia. In flax fibres, kink-bands modify the aesthetics and regularity of the fibres, and are also considered as zones of weakness, especially when utilized in a fibre-reinforced composite[29]. Kink-bands also make the fibre more susceptible and sensitive to ageing by acting as entry points for microorganisms or moisture to access the inner layers of the cell walls[30].

We specifically examined the kink-bands through multiphoton microscopy with second harmonic generation (SHG) imaging, which highlighted crystalline cellulose within the plant cell walls. Figure 3c shows discontinuity and disorganization of crystalline cellulose in the kink-band of old flax, which possibly indicate areas of low crystallinity in this region. Both these factors would cause kink-band-rich ancient flax fibres to be more brittle[13]. Indeed,

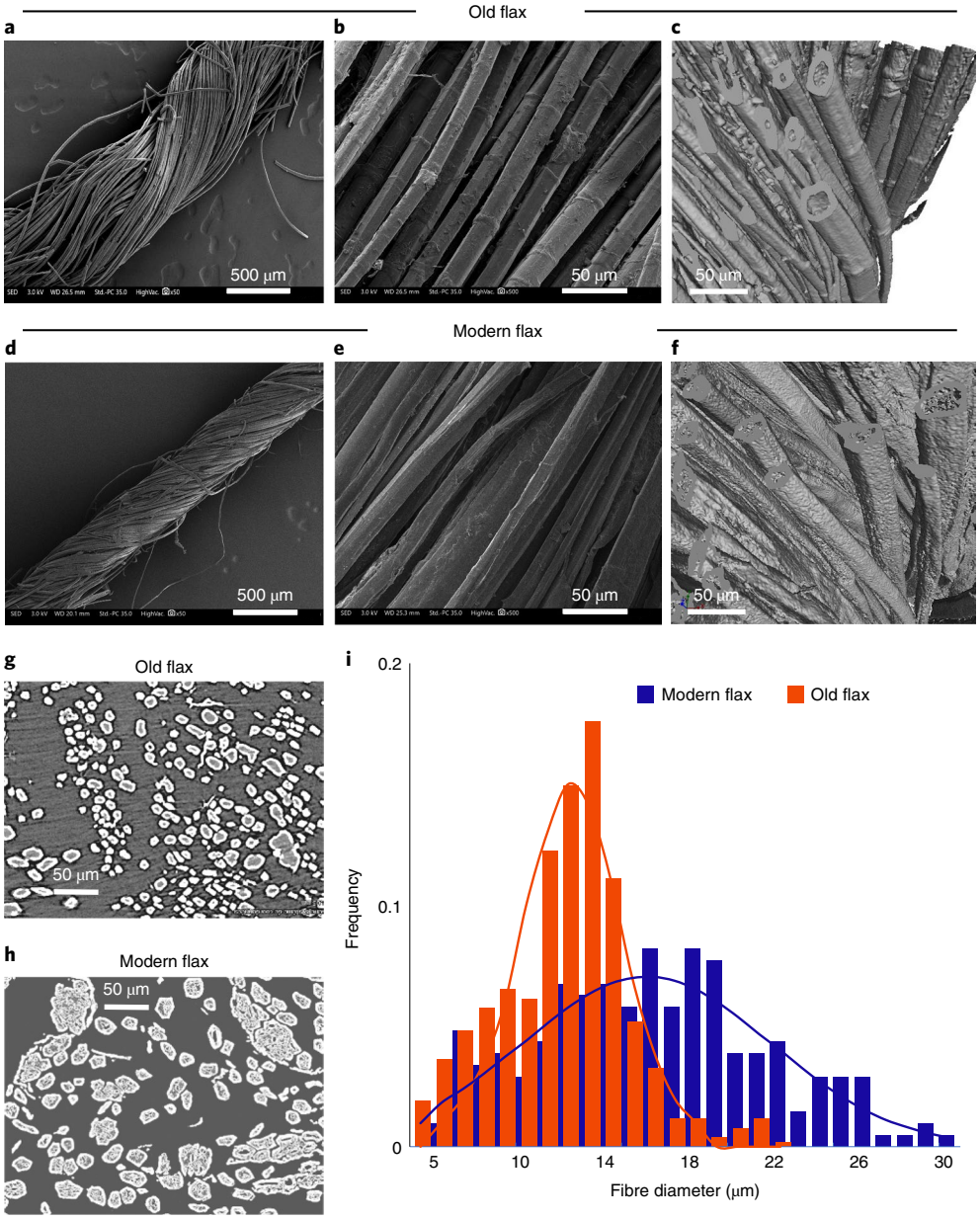

Fig. 2 | SEM and nano-tomography images of modern and 4,000-year-old flax. a–**h**, Overview of yarn (**a**,**d**) and fibres within the yarns (**b**,**e**); tomographic overview of fibres highlighting the larger lumen size of old flax (**c**,**f**) and tomographic yarn cross-section showing the smaller diameter of old flax fibres (**g**,**h**). **i**, Histograms of the distribution of single-fibre diameters for both old and modern flax. For SEM, at least five areas were investigated and the most representative images selected for publication; nano-tomographic images were acquired from a measured volume of 0.5 mm in diameter over a height of 0.8 mm and each projection obtained was the result of the averaging of 15 acquisitions. More images and raw data are available at https://doi.org/10.17863/CAM.72394.

these old fibres have proved to be very fragile during handling, and impossible to isolate without breaking/damaging them for any single-fibre tensile testing.

Finally, atomic force microscopy tests in peak force quantitative nano-mechanical (AFM-PF-QNM) mode were conducted on transverse cross-sections of old and modern flax fibres. Such measurements (Fig. 4) allow estimation of the indentation modulus of flax plant cell walls, that is, they do not depend on the relative lumen size and are a useful measure for highlighting mechanical property gradients or heterogeneities within cell walls[31]. Interestingly, we found that the AFM mechanical properties are slightly higher for cell walls of old flax (23.7 ± 0.2 GPa) than those of modern flax (20.3 ± 0.1 GPa); for each batch, 2,500 indentation modulus values were statistically compared and the Student's *t*-test confirmed that the two sets of moduli are different, with $P \leq 0.001$. Values for modern flax are in line with measurements in the literature[25] as measured by nanoindentation (Supplementary Table 1). Measurements by infrared spectroscopy (Supplementary Fig. 1 and Table 2) revealed a lower intensity of peaks attributed to parietal hemicelluloses in old flax. It has been shown that the longitudinal and transverse shear moduli of the fibres[32] and especially the stiffness of the non-cellulosic matrix of the plant cell walls[33] have a major effect on the indentation modulus; our results confirm this important influence of hemicelluloses on the indentation modulus, even though hemicelluloses are the softest component of the cell wall. Higher indentation moduli have previously been recorded on old

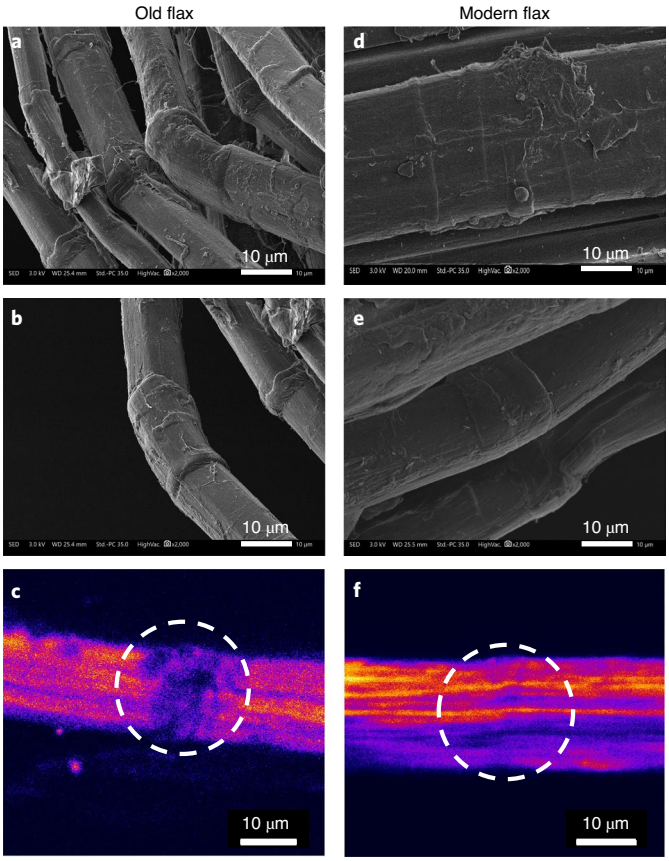

Fig. 3 | Focus on kink-band (defect) regions in the fibres. a–**f**, SEM images showing differences between kink-band structure and intensity in old (**a**,**b**) and modern (**d**,**e**) flax. SHG microscopy observations highlight the local disorganization of cellulose macrofibrils in the kink-band region for old flax (**c**) compared with modern flax (**f**). In **c** and **f**, kink band regions are circled by the dotted white line. For SEM and SHG, at least five areas were investigated and the most representative images selected for publication. More SEM images and raw SHG data are available at https://doi.org/10.17863/CAM.72394.

wood samples and are attributed to a loss of pectins, as well as modification of the ligno-cellulosic cell wall polymers[34]. The wider literature supports the hypothesis of a significant evolution in ageing sensitive hemicellulosic polymers over 4,000 years old. Differences in crystallinity were also checked through both nuclear magnetic resonance (NMR) and X-Ray diffraction (XRD) measurements; Supplementary Fig. 2 shows that the cellulose crystallinity measured by both NMR (58.0% for the old Egyptian yarn and 56.0% for the modern yarn) and XRD (59.6% for Egyptian yarn and 58.4% for modern yarn) techniques was comparable between the ancient and the modern flax yarns. Moreover, the measured indentation moduli were homogeneous in the fibre sections and show little dispersion, suggesting no ageing gradient across a fibre transverse section. Such quantitative nano-structural measurements, never before conducted on such ancient fibres, reveal the durability of these flax plant cell walls. Even though at the fibre-scale, the kink-bands are regions of pronounced damage, the cell walls themselves exhibited a moderate change in their elastic performance despite their age; only a slight increase in their stiffness, connected to the evolution of their non-cellulosic polysaccharide composition, was demonstrated.

Our structural examination of 4,000-year-old Egyptian flax fibres in comparison with modern flax fibres has offered several insights on the textile know-how of the Egyptians, as well as on the temporal evolution of flax fibres. Through water-retting and manual processing, the ancient Egyptians could separate the flax into very fine fibre bundles and in most cases, even into single fibres to make soft and luxurious quality textiles despite fully manual processing. Local nano-mechanical measurements show an increase in cell wall stiffness in old fibres, probably induced by the alteration of non-cellulosic polymers, as cellulose retained a crystallinity close to that of contemporary fibres. In addition, a larger presence of structural defects – stress-concentrating kink-bands with low cellulose crystallinity – is notable on the old, fragile fibres. In future and in current work, we aim to go further by exploring the microfibrils angle values of ancient flax (through single-fibre XRD and SHG), the internal structure of kink-bands (by nano-tomography) and if possible, to gain information on the *Linum* used by ancient Egyptians through genetic analysis. To improve durability at the fibre scale, producing fibres with low quantities of defects is necessary, in particular if they are to be used as reinforcements of next-generation environmentally friendly composite materials. Intriguingly, the ancient Egyptians had also dabbed their hands in making the first linen/plaster cartonnage biocomposites for death masks, a number of which survive to date (Fig. 1b).

Methods

Materials. Two samples of flax yarns were studied (Supplementary Fig. 3), an ancient and a contemporary sample, referred to as old and modern flax, respectively. The large linen tabby, bordered with a fringe (inv. E 13595, Supplementary Fig. 3a) was given in 1929 by Georges Daressy, former General Secretary of the Antiquity Service in Egypt, to the Louvre Museum. Its provenance is unknown, but this piece of shroud most probably came from a tomb because all the textiles of ancient Egypt were found in cemeteries. These cemeteries were located in the desert to ensure dryness and optimal conservation of the burials. Indeed, in the valley, the annual flooding of the Nile was too risky. Thus, the Egyptian climate of the desert areas, which was exceptionally dry and favourable to the proper conservation of organic materials, made it possible to find many fabrics in excellent condition. The linen was radiocarbon dated in 2009 (Laboratoire de Mesure du Carbone 14, CEA-Saclay, France): it had been collected between 2140 and 1976 BC (with 95.4% probability), during the 9th, 10th or 11th dynasties, a period known as the First Intermediate Period and the beginning of the Middle Egyptian Kingdom. Morphological characteristics of the ancient yarn were calculated from mass measurements and from image analysis. The linear density and twist of this old yarn are 122 tex and 180 tpm, respectively. In addition, a contemporary yarn was used (Supplementary Fig. 3b). It was produced from textile flax (Melina variety) cultivated in 2018 in Normandy (France) by Teillage Saint-Martin company; this flax was dew-retted conventionally over six weeks and then scutched and hackled (Bourmaud et al. 2018 PMS). Then, it was wet spun by Safilin Pionki (Poland), with a linear density and twist of 105 tex and 320 tpm, respectively.

SEM observations. For each of the two yarns, a sample of a few millimetres was used. A Jeol JSM 6460LV scanning electron microscope was used to analyse the flax yarns; secondary emission electrons were used and the accelerating voltage was 3.0 kV. The yarn samples were glued to a sample holder using a conductive adhesive and then metallized with a thin layer of gold using an Edwards Scancoat Six device for 180 s.

Multiphoton microscopy. *Preparation of samples.* An elementary fibre was extracted from the modern flax yarn and mounted on paper support commonly used for tensile tests according to ASTM C1557 and fixed with universal glue. The sample prepared was placed between two coverslips and scanned. In contrast, the preservation state of the Egyptian yarn did not allow the extraction of elementary fibres, which were more brittle, so a whole collective of less than 1 cm was mounted on paper support commonly used for tensile tests but glued in the horizontal direction to use the aperture of 5 mm. The sample prepared was placed between two coverslips and scanned by the multiphoton microscope. The samples were mounted at 90° to the initial laser polarization position.

SHG microscopy imaging. SHG imaging was performed with a multiphoton Nikon A1 MP+ microscope (NIKON) equipped with a long working distance 16× (NA 0.80) water immersion objective (NIKON). The system is equipped with a tunable Mai Tai XF mode-locked Ti:sapphire femtosecond laser (SPECTRA PHYSICS) and a half-wave plate (MKS) in front of the laser excitation beam. The half-wave plate was rotated to change the laser polarization angle to reach the maximum intensity SHG signal of both flax yarns (maximum signal reached 2–3°). The excitation wavelength chosen was 810 nm (average power at 1.5 W) to obtain the maximum performance from the equipped filters (SH collected with a bandpass filter at 406/15 nm), and the maximum laser power percentage used was 2% for

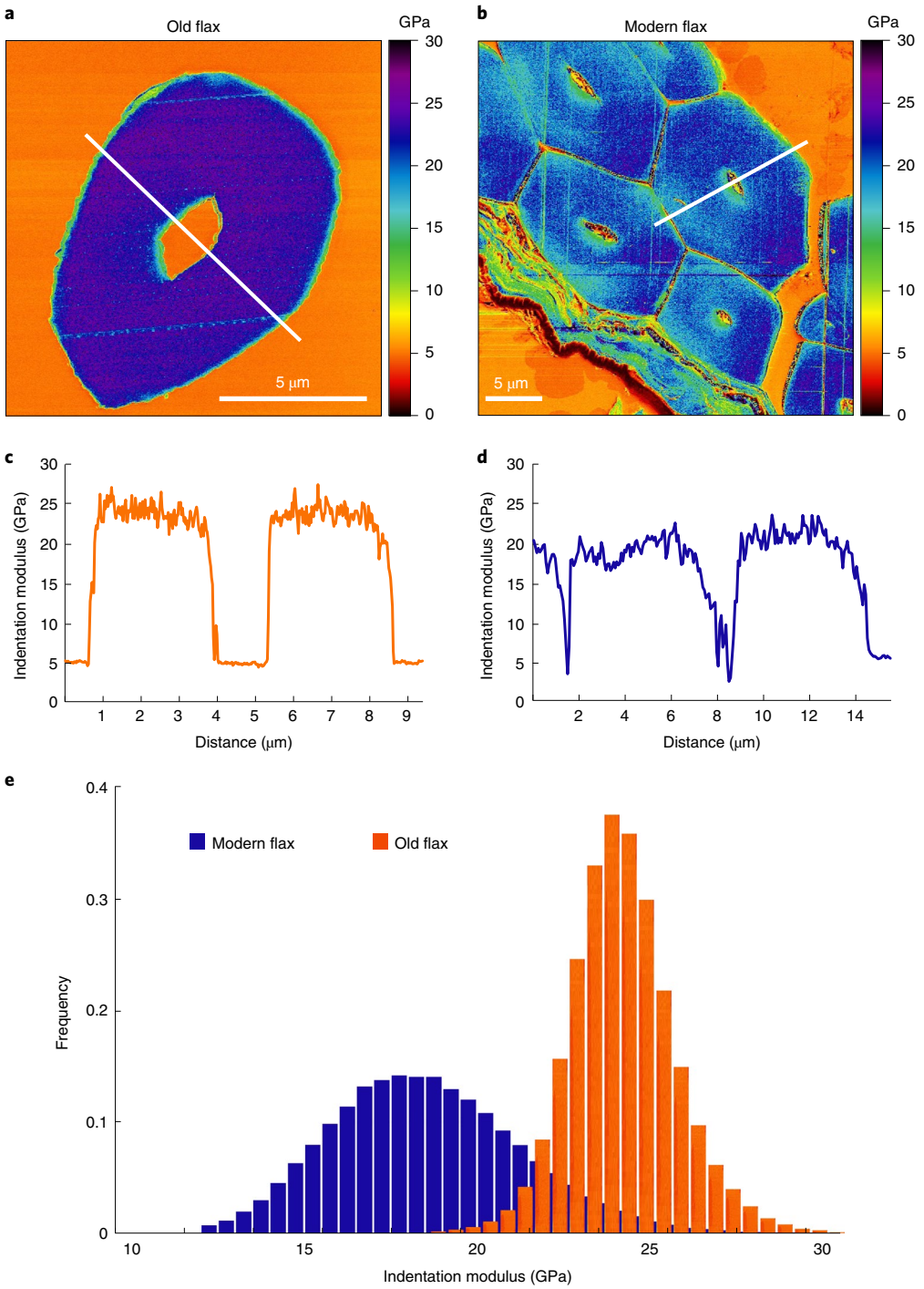

Fig. 4 | AFM peak force measurements in old and modern flax fibres. a,**b**, One can observe larger lumen size on old flax fibre (**a**) and residue of cortical parenchyma on modern flax (**b**). **c**,**d**, Profile of indentation moduli in old (**c**) and modern (**d**) flax based on the position on the white line in **a** and **b**. **e**, Distributions of indentation moduli, which are in good agreement with the preliminary nanoindentation tests performed (Supplementary Table 1).

the Egypt yarn and 5% for the modern yarn to avoid bleaching of the surface. We collected both autofluorescence and SHG signals by GaAsP NDD (gallium arsenide non-descanned) detectors. The scan line average was 16, the scan velocity was fixed at 1 (fps) and the scan size was 512×512 pixels. All the measurements were performed at room temperature and dry ambient conditions.

X-ray tomography measurements. The yarns' microstructure was characterized using X-ray nano-tomography. Image acquisition was realized on an EasyTom micro/nano-tomograph (RX Solutions). A Lanthanum hexaboride (LaB6) filament was used as cathode with a voltage of 50 keV and a current of 100 µA, leading to a resolution of 0.5 µm. The anode was in beryllium and has a thickness of 0.5 mm. Resolution of the micro-CT images was set to 4.44 µm per pixel.

The imager used was a fluoroscopic high speed imaging sub-system PaxScan 2520DX and the scintillator was produced with a direct deposition of cesium iodide. To obtain optimum measurement contrast, the framerate was set to 0.25 fps. In addition, to minimize the measurement noise, each projection obtained was the result of the averaging of 15 acquisitions. Finally, to obtain the most faithful reconstruction possible, the flax fibres were measured in 1,440 different positions (angles). Yarn centering was carried out using a perforated carbon tube. The tube outside diameter was 1 mm and the inside hole diameter was 0.5 mm. A little bit of glue was used to maintain the yarns. The measured volume was 0.5 mm in diameter over a height of 0.8 mm, with a resolution of 500 nm. To allow maximum beam stability from the start of the measurement, the wire was preheated 3 h before the start of the measurement. In total, each measurement therefore lasted

approximately 27 h. An X-ray radiograph is given in Supplementary Fig. 4a to illustrate the measurement (the yarn is hardly perceptible). The reconstruction was carried out with Xact software using the filtered back-projection method. For noise filtering, the apodization was done using a sine window with a threshold of 75% for the low-pass filter. For the border filter, a Tukey window type was used with a non-filtered area of 46%. For more information on filters and the effects of reconstruction filter on cone beam computed tomography (CBCT) image quality, see ref. [35]. Once the reconstruction had been carried out, the result was stored in the form of a slices stack. An illustration is given in Supplementary Fig. 4b. Finally, the analyses and reconstruction of surfaces were carried out using the VGSTUDIO MAX software as illustrated in Supplementary Figs. 5a,b at two different scales.

Nano-mechanical investigations. *Preparation of samples.* A subsample of less than 1 cm was cut from the ancient flax yarn (Louvre) and modern flax yarn samples. The two subsamples were put in an oven at 60 °C for 2 h and then embedded in Agar resin (epoxy resin Agar Low Viscosity Resin, Agar Scientific). The blocks prepared were put back in the oven at 60 °C overnight for the final polymerization of the resin, then machined to reduce their cross-section and glued on a 12 mm AFM stainless steel mounting disk. The sample surface was then cut using an ultramicrotome (Ultracut S, Leica Microsystems) equipped with diamond knives (Histo and Ultra AFM, Diatome) to obtain thin sections (about 50 nm thick in the last step) at reduced cutting speed (~1 mm s^{-1}) to minimize compression and sample deformation during the cutting process, and thus reduce the sample surface damage and topography (Supplementary Fig. 6).

AFM PF-QNM investigations. A Multimode 8 Atomic Force microscope (Bruker) was equipped with a RTESPA-525 probe (Bruker) with a nominal spring constant of 200 N m^{-1} and a resonance frequency of 525 kHz. The actual spring constant was calculated with the Sader Method (https://sadermethod.org/). The AFM set-up was calibrated with the relative method using sapphire as hard standard material to calculate the deflection sensitivity and the PF-QNM synchronization distance. A sample of aramid fibres K305 Kevlar Taffetas (305 g m^{-2}, Sicomin Epoxy Systems) accurately prepared in blocks of Agar resin (Agar Low Viscosity Resin, Agar Scientific), with the surface prepared using the same protocol as that of the flax samples, was previously tested by nanoindentation and then used to calibrate the tip radius (aramid fibre ~24.3 GPa and embedded resin ~5.4 GPa). The range of stiffness of the cantilevers used was between 109 and 161 N m^{-1} and the tip radius between 15 and 30 nm at the beginning of the measurements.

The fast scan axis angle was 90°, the maximum of the peak force setpoint used was 200 nN, the oscillation frequency selected at 2 kHz and the Poisson's ratio used was set to 0 as the tested cell walls are anisotropic, thus the modulus measured is the indentation modulus. The maximum fast scan velocity was selected at 8 µm s^{-1} and the image resolution set to 512 × 512 pixels. The gain was set in automatic mode.

Two to three different areas of each sample (old and modern, respectively) were measured to obtain a better statistic, but only one representative area for each sample is reported here (Fig. 4 and Supplementary Figs. 6 and 7). Supplementary Fig. 6 shows the topography images corresponding to investigated areas of Fig. 4. To obtain the indentation modulus values, the entire surface of the secondary S_2 (or G) wall of each fibre was selected; indentation modulus data were automatically calculated for each point from the force–distance curves with a Derjaguin–Muller–Toporov (DMT) contact model using NanoScope Analysis software (Bruker).

Consequently, for each sample, the indentation moduli calculated were obtained from two or three separate images and from between 80,000 and 140,000 points for each image analysed using Gwyddion free software (http://gwyddion.net/). Supplementary Fig. 7 shows the calculation mask, covering the investigated area for fibres in Fig. 4. For each sample, histograms in Fig. 4 represent the data obtained from all the images analysed; 206,613 and 364,575 AFM force curves were used for old and modern flax indentation modulus calculation, respectively.

Statistical analysis. A Student's *t*-test was performed to quantify the statistical differences in fibre diameters and indentation modulus values between the old and the modern fibres. A *P* value was calculated for the two cases, with significance level $\alpha = 0.05$.

Reporting Summary. Further information on research design is available in the Nature Research Reporting Summary linked to this article.

Data availability

The data that support the plots within this paper and the findings of this work are available from the corresponding author and at the following address: https://doi.org/10.17863/CAM.72394. Source data are provided with this paper.

Code availability

The open-source and commercial software used for data analysis are referenced in the Methods section.

References

1. van Zeist, W. & Bakker-Heeres, J. A. H. Evidence for linseed cultivation before 6000 bc. *J. Archaeol. Sci.* **2**, 215–219 (1975).
2. Hopf, M. in *The Domestication and Exploitation of Plants and Animals* (ed. Dimbleby, G.) Pt. III, Ch. 6 (2008).
3. Herbig, C. & Maier, U. Flax for oil or fibre? Morphometric analysis of flax seeds and new aspects of flax cultivation in late Neolithic wetland settlements in southwest Germany. *Veg. Hist. Archaeobot.* **20**, 527 (2011).
4. Kvavadze, E. et al. 30,000-year-old wild flax fibers. *Science* **325**, 1359 (2009).
5. Heer, O. Prehistoric culture of flax. *Nature* **7**, 453 (1873).
6. le Duigou, A. & Castro, M. Evaluation of force generation mechanisms in natural, passive hydraulic actuators. *Sci. Rep.* **6**, 18105 (2016).
7. Mohanty, A. K., Vivekanandhan, S., Pin, J.-M. & Misra, M. Composites from renewable and sustainable resources: challenges and innovations. *Science* **362**, 536–542 (2018).
8. Bruni, S. et al. Analysis of an archaeological linen cloth: the shroud of Arquata. *Radiat. Phys. Chem.* **167**, 108248 (2020).
9. Edwards, H. G. M., Ellis, E., Farwell, D. W. & Janaway, R. C. Preliminary study of the application of Fourier Transform Raman Spectroscopy to the analysis of degraded archaeological linen textiles. *J. Raman Spectrosc.* **27**, 663–669 (1996).
10. Kavkler, K., Gunde-Cimerman, N., Zalar, P. & Demšar, A. FTIR spectroscopy of biodegraded historical textiles. *Polym. Degrad. Stab.* **96**, 574–580 (2011).
11. Kavkler, K., Šmit, Ž., Jezeršek, D., Eichert, D. & Demšar, A. Investigation of biodeteriorated historical textiles by conventional and synchrotron radiation FTIR spectroscopy. *Polym. Degrad. Stab.* **96**, 1081–1086 (2011).
12. Müller, M. et al. Identification of ancient textile fibres from Khirbet Qumran caves using synchrotron radiation microbeam diffraction. *Spectrochim. Acta Part B At. Spectrosc.* **59**, 1669–1674 (2004).
13. Herrera, L. K. et al. Identification of cellulose fibres belonging to Spanish cultural heritage using synchrotron high resolution X-ray diffraction. *Appl. Phys. A* **99**, 391–398 (2010).
14. Weiss, E. & Zohary, D. The Neolithic southwest Asian founder crops: their biology and archaeobotany. *Curr. Anthropol.* **52**, S237–S254 (2011).
15. Botany of flax. *Nature* **170**, 557–559 (1952).
16. Sertse, D., You, F. M., Ravichandran, S. & Cloutier, S. The genetic structure of flax illustrates environmental and anthropogenic selections that gave rise to its eco-geographical adaptation. *Mol. Phylogenet. Evol.* **137**, 22–32 (2019).
17. Braun, A. Plants of ancient Egypt. *Sci. Am.* **173**, 2760 (1879).
18. Diederichsen, A. & Hammer, K. Variation of cultivated flax (*Linum usitatissimum* L. subsp. *usitatissimum*) and its wild progenitor pale flax (subsp. *angustifolium* (Huds.) Thell.). *Genet. Resour. Crop Evol.* **42**, 263–272 (1995).
19. Kawami, T. S. A craft in antiquity. *Science* **256**, 1065–1066 (1992).
20. André, J. in *Pline l'Ancien, Histoire naturelle* (ed. Budé, G.) 549–550 (1964).
21. Goudenhooft, C., Bourmaud, A. & Baley, C. Varietal selection of flax over time: evolution of plant architecture related to influence on the mechanical properties of fibers. *Ind. Crops Prod.* **97**, 56–64 (2017).
22. Baley, C. & Bourmaud, A. Average tensile properties of French elementary flax fibers. *Mater. Lett.* **122**, 159–161 (2014).
23. Chemikosova, S. B., Pavlencheva, N. V., Gur'yanov, O. P. & Gorshkova, T. A. The effect of soil drought on the phloem fiber development in long-fiber flax. *Russ. J. Plant Physiol.* **53**, 656–662 (2006).
24. Bourmaud, A., Gibaud, M., Lefeuvre, A., Morvan, C. & Baley, C. Influence of the morphology characters of the stem on the lodging resistance of Marylin flax. *Ind. Crops Prod.* **66**, 27–37 (2015).
25. Bourmaud, A., Beaugrand, J., Shah, D., Placet, V. & Baley, C. Towards the design of high-performance plant fibre composites. *Prog. Mater. Sci.* **97**, 347–408 (2018).
26. Goudenhooft, C., Bourmaud, A. & Baley, C. Study of plant gravitropic response: exploring the influence of lodging and recovery on the mechanical performances of flax fibers. *Ind. Crops Prod.* **128**, 235–238 (2019).
27. Hernandez-Estrada, A., Gusovius, H.-J., Müssig, J. & Hughes, M. Assessing the susceptibility of hemp fibre to the formation of dislocations during processing. *Ind. Crops Prod.* **85**, 382–388 (2016).
28. Hughes, M. Defects in natural fibres: their origin, characteristics and implications for natural fibre-reinforced composites. *J. Mater. Sci.* **47**, 599–609 (2012).
29. Le Duc, A., Vergnes, B. & Budtova, T. Polypropylene/natural fibres composites: analysis of fibre dimensions after compounding and observations of fibre rupture by rheo-optics. *Compos. Part A Appl. Sci. Manuf.* **42**, 1727–1737 (2011).
30. Foulk, J., Akin, D. & Dodd, R. Influence of pectinolytic enzymes on retting effectiveness and resultant fiber properties. *BioResources* **3**, 155–169 (2008).
31. Eder, M., Arnould, O., Dunlop, J. W. C., Hornatowska, J. & Salmen, L. Experimental micromechanical characterisation of wood cell walls. *Wood Sci. Technol.* **47**, 163–182 (2012).

32. Jäger, A., Bader, T., Hofstetter, K. & Eberhardsteiner, J. The relation between indentation modulus, microfibril angle, and elastic properties of wood cell walls. *Compos. Part A Appl. Sci. Manuf.* **42**, 677–685 (2011).
33. Capron, M. et al. Mechanical characterization of developing tension wood fibre wall by atomic force microscopy. In *8th Plant Biomechanics International Conference* 224–225 (Nagoya, 2015).
34. Bader, T. K., de Borst, K., Fackler, K., Ters, T. & Braovac, S. A nano to macroscale study on structure–mechanics relationships of archaeological oak. *J. Cult. Herit.* **14**, 377–388 (2013).
35. Shaw, C. *Cone Beam Computed Tomography* (Taylor & Francis, 2014).

Acknowledgements

V.P. and G.H. sincerely thank P. Malécot and the MIFHySTO research platform (FEMTO-ST, UTINAM and ICB institutes) at Université Bourgogne Franche-Comté (UBFC) for the technical and scientific support provided for nano-tomography experiments; X. Falourd and L. Foucat (INRAE, BIBS platform) for NMR investigations. We thank the INTERREG IV Cross Channel programme for funding this work through the FLOWER project (grant no. 23); SOLEIL Synchrotron for funding the 99180266 and 99200015 in-house proposals; and the EIPHI Graduate school (contract "ANR-17-EURE-0002").

Author contributions

A.B. and D.U.S designed this work. A.M., G.H., O.A., S.D., V.P., J.B., F.J. and A.B. collected and analysed data. A.B., A.M. and D.U.S wrote and revised the paper, with contributions from G.H., R.C., O.A., V.P., D.B., S.D., J.B. and F.J.

Competing interests

The authors declare no competing interests.

Additional information

Supplementary information The online version contains supplementary material available at https://doi.org/10.1038/s41477-021-00998-8.

Correspondence and requests for materials should be addressed to Alain Bourmaud.